Integrative and Comparative Biology

Integrative and Comparative Biology, pp. 1–13
doi:10.1093/icb/icz141

Society for Integrative and Comparative Biology

SYMPOSIUM

Hurry Up and Get Out of the Way! Exploring the Limits of Muscle-Based Latch Systems for Power Amplification

Emily M. Abbott,* Teron Nezwek,† Daniel Schmitt† and Gregory S. Sawicki[1,*]

*George W. Woodruff School of Mechanical Engineering and School of Biological Sciences, Georgia Institute of Technology, 801 Ferst Drive, GA 30332-0405, USA; †Department of Evolutionary Anthropology, Duke University, Durham, NC 27708-9976, USA

From the symposium "Playing with Power: Mechanisms of Energy Flow in Organismal Movement" presented at the annual meeting of the Society for Integrative and Comparative Biology, January 3–7, 2019 at Tampa, Florida.

[1]E-mail: gregory.sawicki@me.gatech.edu

Synopsis Animals can amplify the mechanical power output of their muscles as they jump to escape predators or strike to capture prey. One mechanism for amplification involves muscle–tendon unit (MT) systems in which a spring element (series elastic element [SEE]) is pre-stretched while held in place by a "latch" that prevents immediate transmission of muscle (or contractile element, CE) power to the load. In principle, this storage phase is followed by a triggered release of the latch, and elastic energy released from the SEE enables power amplification ($P_{RATIO}=P_{LOAD}/P_{CE,max} > 1.0$), whereby the peak power delivered from MT to the load exceeds the maximum power limit of the CE in isolation. Latches enable power amplification by increasing the muscle work generated during storage and reducing the duration over which that stored energy is released to power a movement. Previously described biological "latches" include: skeletal levers, anatomical triggers, accessory appendages, and even antagonist muscles. In fact, many species that rely on high-powered movements also have a large number of muscles arranged in antagonist pairs. Here, we examine whether a decaying antagonist force (e.g., from a muscle) could be useful as an active latch to achieve controlled energy transmission and modulate peak output power. We developed a computer model of a frog hindlimb driven by a compliant MT. We simulated MT power generated against an inertial load in the presence of an antagonist force "latch" (AFL) with relaxation time varying from very fast (10 ms) to very slow (1000 ms) to mirror physiological ranges of antagonist muscle. The fastest AFL produced power amplification ($P_{RATIO}=5.0$) while the slowest AFL produced power attenuation ($P_{RATIO}=0.43$). Notably, AFLs with relaxation times shorter than ~300 ms also yielded greater power amplification ($P_{RATIO}>1.20$) than the system driving the same inertial load using only an agonist MT without any AFL. Thus, animals that utilize a sufficiently fast relaxing AFL ought to be capable of achieving greater power output than systems confined to a single agonist MT tuned for maximum P_{RATIO} against the same load.

Introduction

Animals that rely on rapid movement for survival produce high rates of acceleration despite the relatively slow speed of muscular contraction (Bennet-Clark and Lucey 1967; Gronenberg 1996; Wilson et al. 2003; Vogel 2005). To accelerate quickly, animals use diverse strategies that decrease the amount of time or increase the amount of energy stored, required to perform a given amount of mechanical work, thus increasing power (power = work/time = force× velocity). We consider a movement to exhibit power amplification (P_{AMP}), when the observed power output exceeds the maximal power that could be achieved through muscular contraction alone (i.e., $P_{RATIO} = P_{LOAD}/P_{CE,max} > 1.0$). For the purposes of this paper, the term "power amplification" does not reflect additional contributions of energy.

Power amplification (P_{AMP}) is common and important for animal movement. Two well characterized examples of power amplification are jumping frogs and striking shrimp. Frogs accelerate their bodies through limb extension; and their relatively long legs provide more time for acceleration while

animals with short limbs have a limited acceleration period (Vogel 2005). Yet, if an animal wishes to escape quickly, there may be serious limitations of directly powering a movement with muscle due to Hill-type force–velocity properties. Muscular force decreases significantly as a function of the shortening speed. Thus, in the quickest movements extensor muscles may not produce enough mechanical work to move a respectable absolute distance. Evidence suggests that frogs overcome some limitations of their muscle shortening speed through the use of a catapult-like mechanism in which the muscle–tendon (MT) unit releases energy faster than it was stored (Marsh 1994; Peplowski and Marsh 1997; Astley and Roberts 2012). Likewise, during predatory strikes, the peacock mantis shrimp (*Odontodactylus scyllarus*) generates incredibly high power outputs using a latch mechanism to allow for the slow storage and rapid release of elastic energy (Patek et al. 2004, 2007). Similar power amplification mechanisms, where energy is stored before a quick movement, are also manifest in trap jaw ants biting (Gronenberg et al. 1993; Patek et al. 2006), insects jumping (Bennet-Clark and Lucey 1967; Bennet-Clark 1975; Burrows 2011; Burrows and Sutton 2012), primates jumping (Aerts 1998), salamanders, and toads capturing prey (Lappin et al. 2006; Deban et al. 2007) and horses sprinting (Wilson et al. 2003).

All these diverse power amplification movements require three elements: a contractile element (CE), a series elastic element (SEE), and a latch. The mechanism of power amplification occurs in three stages: (i) the energy storage phase in which the CE produces force, stretches the SEE, and a biological latch holds the SEE in tension, (ii) the triggered release of the latch, and (iii) the energy release phase in which the SEE recoils and transfers the stored elastic potential energy to a load such as a body or appendage (Roberts and Marsh 2003; Patek et al. 2007; Roberts and Azizi 2011; Astley and Roberts 2012; Lipfert et al. 2014). Because power is a rate of energy release (i.e., work/time), one way animals can achieve power amplification by reducing the time of energy release (stage iii) compared with the time over which energy is stored (stage i). Power is enhanced when the observed power output exceeds the maximal power that could be achieved through muscular contraction alone (i.e., $P_{AMP} = P_{LOAD}/P_{CE,max} > 1$). In principle, when the mechanics of force generation in the CE and the compliance of the SEE are optimally tuned, stored elastic energy will recoil with timing that acts to amplify power output of the MT (Galantis and Woledge 2003; Richards and Sawicki 2012; Rosario et al. 2016).

While power amplifying mechanisms manifest in a broad range of taxa, the specific biological structures differ depending on the species or task. Narrowing our scope to vertebrate terrestrial locomotion, we consider skeletal muscles as the CE. For the SEE component, there are several candidates. A biological spring can be any structure that stretches in response to an applied force, such as from a muscle contraction or an external load. These could include small-scale elastic structures within muscle such as titin (Wang et al. 1993; Rode et al. 2009; Nishikawa et al. 2012; Powers et al. 2017). And, there is an increasing amount of evidence that calcium-activated titin is not simply an elastic element but has important history-dependent effects regarding muscle function (i.e., force enhancement and force depression (Rode et al. 2009; Tomalka et al. 2017). However, *in vivo* data indicate that larger-scale collagenous structures (i.e., connective tissue, tendons, and aponeuroses) are thought to be the primary sources of elastic energy storage used during terrestrial vertebrate locomotion (Alexander 2002; Roberts and Azizi 2011; Roberts 2016). Latches can also come in many forms. For example, previous research has indicated several different latching mechanisms used by animals, such as body-weight, skeletal levers, accessory appendages, trigger structures, and even antagonistic muscles (Heitler 1974; Bennet-Clark 1975; Gronenberg 1996; Roberts and Marsh 2003).

Despite the large variation, research into how latch form and function influences mechanical energy flow in locomotion systems is limited. The purpose of this study was to employ a modeling and simulation framework to explore the factors that determine whether antagonist muscles can serve as effective latch systems to enable high peak power and acceleration of an inertial load. Muscles arranged in antagonist pairs are found widely across species and have been shown to be critical for allowing functional control of joint position and stiffness (Hogan 1985; Farahat and Herr 2010). It is also possible that coordinated action of antagonist muscle pairs may enable controlled energy flow during high-power movements (Gronenberg 1996). For example, co-activation of an agonist–antagonist muscle pair (storage—stage i) followed by fast relaxation of the antagonist muscle (release—stage iii) could yield power amplification.

A recent modeling and simulation study examined how the geometry of an anatomical latch can substantially affect ballistic performance of a spring-powered load (Ilton et al. 2018). Specifically, Ilton et al. (2018) demonstrated that latches with instantaneous escapement (i.e., discrete energy storage and

release phases) achieve the highest peak power and acceleration of an inertial load, while latches with interference tend to slow the release of energy and limit peak performance. Similarly we sought to investigate the "gray zone" between discrete energy storage and release phases when the latch is a generalized, decaying antagonist force. We asked: Can antagonist forces that un-latch on a timescale similar to skeletal muscle relaxation still enhance power transferred to a load? We hypothesized that, when driving an inertial load: (1) there is a critical un-latching time where a MT system with an antagonist muscle latch matches the peak power output of the system without a latch and that (2) un-latching times that are faster/slower than the critical un-latching time enhance/attenuate peak power. To our knowledge, no current literature has produced a general model of an antagonist–latch mechanism (muscle or otherwise) that can be applied broadly across species and ballistic movements.

Materials and methods

To investigate how latch dynamics influence mechanical power transfer from a MT unit to inertial load we modified a Hill-type muscle model used by Richards and Sawicki (2012) to include an antagonist force latch (AFL). Following prior work (Galantis and Woledge 2003; Richards and Sawicki 2012), the agonist MT consisted of a CE connected in series with an idealized Hookean elastic element (SEE). Schematically, the MT generated a force on an inner pulley (radius = L_{in}) that resulted in load transmission across a larger pulley (radius = L_{out}). We located the AFL on the inner pulley opposite the MT to negate any influence of effective mechanical advantage between the antagonist pair. Next, we mathematically designed a latch that generated the same amount of force as the MT during the storage phase. Because the latch was a perfect antagonist, all of the agonist energy was stored in the SEE. We did not model the SEE as nonlinear like many studies that use models to predict motion (van Soest and Bobbert 1993; Delp and Loan 2000). This nonlinearity was not considered because our simulated contractions occurred at high muscle forces where linear and nonlinear elastic elements would behave similarly. During the release phase, the latch force decayed to zero in sigmoidal fashion with duration t_n that varied across simulations (Fig. 1B). During the release phase, MT energy could either be transferred to the load or dissipated by the latch. This novel computational framework is a simplified representation of agonist–antagonist muscle pair that can transfer net energy across a joint to an inertial load (i.e., mass *only*) (Fig. 1). We chose the un-latch time duration t_n as the independent variable of study with the aim to characterize the critical antagonist force un-latch time for power amplification.

The equations of motion used in the MATLAB simulation were taken from Richards and Sawicki (2012) and adjusted to include the force contribution from the AFL. Following Newton's Second Law of Motion, we devised a linear momentum balance equation on the inertial load according to the diagram in Fig. 1 to give Equation (1):

$$F_{LOAD} = ma, \quad (1)$$

where F_{LOAD} is the overall force applied to the load, m is the mass of the load, and a is the acceleration of the load.

We then modified the Richards and Sawicki's (2012) angular momentum balance equation about the massless pulley to include the torque contributed by the AFL, yielding Equation (2):

$$(F_{MT}L_{in}) - (F_{LATCH}L_{in}) - (F_{LOAD}L_{out}) = 0, \quad (2)$$

where L_{in} is the moment arm of both the MT (F_{MT}) and latch (F_{LATCH}) force, and L_{out} is the moment arm of the load force, F_{LOAD}. Because the MT and latch were applied at the same distance from the pulley center, we derived a simplified equation for F_{LOAD} (Equation 3), using the EMA of the MT, a dimensionless lever arm ratio (i.e., EMA = L_{in}/L_{out}):

$$F_{LOAD} = (F_{MT} - F_{LATCH})\text{EMA}. \quad (3)$$

The force generated by the MT is developed by a CE in series with an elastic element (SEE), yielding Equation (4):

$$F_{MT} = F_{CE} = F_{SEE}. \quad (4)$$

The MT in the simulations included physiological and morphological properties of a common frog model (i.e., *Xenopus laevis*) plantaris longus (PL) MT. Each simulation was a singular MT contraction initiated by a maximum intensity square wave excitation to the CE. The CE force was computed using a Hill-type model with first order activation dynamics and non-linear force–velocity properties (Richards and Sawicki 2012). Similar to other baseline modeling studies (Galantis and Woledge 2003; Richards and Sawicki 2012), none of the simulations include CE force–length effects. Using standard equations for shortening (Equation 5), we modeled force–velocity dynamics (Hill, 1938):

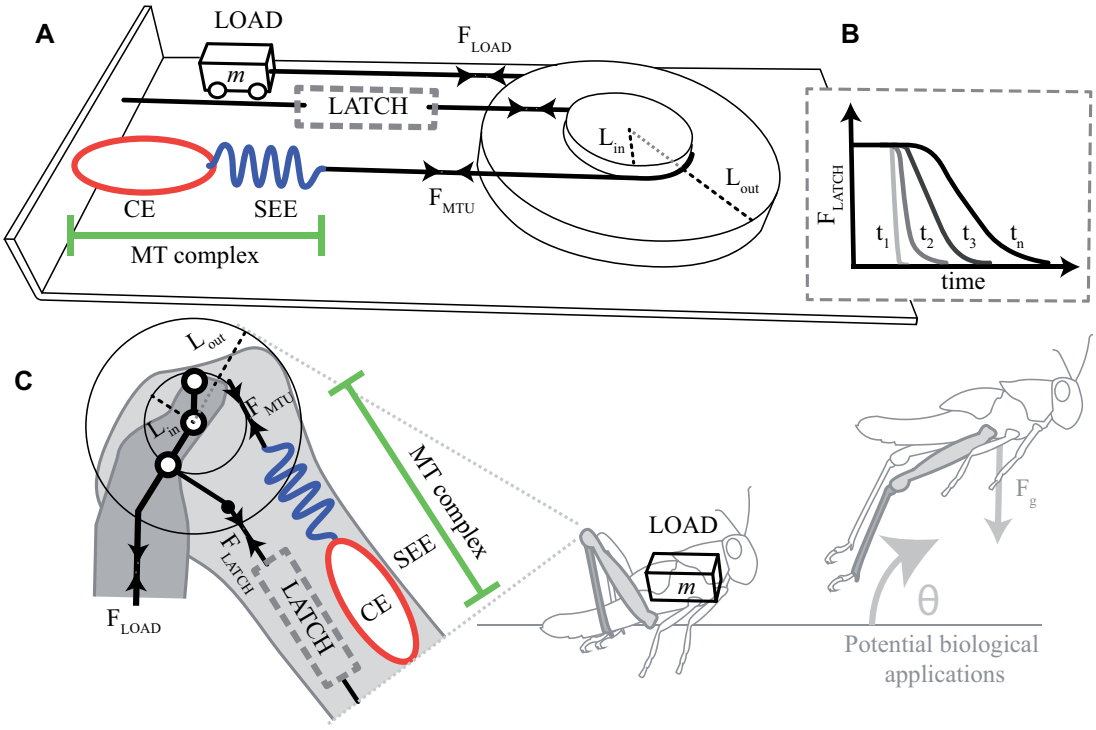

Fig. 1 Schematic diagram illustrates (**A**) an agonist muscle–tendon (MT) unit complex made up of a contractile element (CE) (red) and series elastic element (SEE) (blue) and an antagonist force latch (AFL) connected via a pulley transmission system to an inertial load (m). In the storage phase, the MT complex (F_{MT}) and the AFL (F_{LATCH}) generate equal forces about the small pulley with radius L_{in}, placing the system in static equilibrium. This allows the CE contraction to store significant energy in the SEE. In the release phase, the MT continues to contract and the AFL un-latches, allowing some force/energy to be transmitted the load (F_{LOAD}) via the large pulley with radius L_{out}. Schematic diagram (**B**) describes how F_{LATCH} develops as a function of time for AFLs with un-latch dynamics ranging from very fast (t_1=10 ms) to very slow (t_n=1000 ms). Schematic diagram (**C**) describes how the mathematical model could be applied explicitly to a biological system, such as a grasshopper, with some minor modifications (e.g., the addition of a gravitational component to the load as would be experienced in jumping) Knee diagram adapted from Cofer et al. (2010).

$$F_{MT}(V_{ce}) = \frac{(1 - V_{ce}/V_{max})}{[1 + V_{ce}/(0.25V_{max})]}. \quad (5)$$

Based on prior *in vivo* studies of *X. laevis*, the model employed parameters as follows: maximum isometric muscle force, $F_{CE,max}$ (10.0 N), rest length (20.0 mm), and maximum shortening velocity, V_{max}, of nine muscle rest lengths per second or 180 mm/s (Richards 2011). From these values, we derived the maximum CE power output ($P_{CE,max}$ = 171.9 mW), which occurs at a velocity of about 1/3 $V_{CE,max}$. This power output of the muscle agreed with the predicted $P_{CE,max}$ region in a Hill-type force–velocity curve (Hill, 1938). We set the SEE spring stiffness (1250 N/m), EMA (0.1), and mass (0.03 kg) to the values that generated maximum peak power output in a previous study (Richards and Sawicki 2012). These conditions represent the ideal "inertial-latch" system in the absence of a latch and allow for controlled comparison with modified configurations that do have a physical latch.

Finally, using MATLAB/Simulink (Mathworks Inc., Natick, MA), we created a range of slopes representing various AFL un-latching times, from nearly instantaneous un-latch time (t_1 = 10 ms) to slower un-latching time (t_n = 1000 ms) (Fig. 1B). Then, over the range of un-latch times, we performed simulations by numerically integrating Equation (1) using the step-wise equations established in Richards and Sawicki (2012) with the addition of latch dynamics described in Equations (2)–(5) to obtain values for latch, load, MT, CE, and SEE force, velocity, and length as a function of time. For each element in the model, we calculated mechanical power (i.e., Power = Force× Velocity) as a function of time. In each simulation, we checked for power amplification, P_{AMP}, when $P_{RATIO} > 1.0$, by computing the ratio of the peak power delivered by the MT to the load (P_{LOAD}) to the maximum power that can be generated by the CE; $P_{RATIO} = P_{LOAD}/P_{CE,max}$. Using this model, we addressed our hypotheses by seeking to identify the threshold un-latch time for

which an AFL can amplify peak power delivered to the load (P_{LOAD}).

Of note, many muscle properties were not included in our model such as the force–length relationship, force enhancement, force depression, fiber type, internal inertia, parallel elasticity, and others. For a complete review of these effects, we point readers to an extensive modeling study by Ross et al. (2018). Our intention in using a basic MT model is to study the mechanism of antagonist muscle pairs in the simplest form to yield fundamental insights.

Results

Patterns of force, velocity, and power with and without an AFL

Patterns of force, velocity, and power in the system with an inertial load *only* (Fig. 2A) and with the addition of an AFL (Fig. 2B) demonstrated that power amplification ($P_{RATIO} > 1.0$; $P_{LOAD} > P_{CE,max} = 172$ mW) is possible both in the absence and presence of an AFL, but the pattern of energy flow is different. In the system without an AFL, the dynamic interaction between the MT and the inertial load enables temporary storage of elastic energy in the SEE that is returned with timing that amplifies the peak power ($P_{LOAD} = 203$ mW; $P_{RATIO} = 1.17 > 1.0$) transmitted by the muscle to the load (Fig. 2A), a phenomenon that has been previously described in detail (Galantis and Woledge 2003; Richards and Sawicki 2012).

In systems with an AFL, MT power is not delivered exclusively to the load. During the storage phase, forces contributed by the AFL and MT were equal in magnitude and opposite in direction. Therefore, all of the energy generated by the CE shortening (positive velocity and power) was stored as strain energy in the SEE as it was stretched (negative velocity and power). In the release phase, energy from the agonist MT was distributed between the load and the AFL (Figs. 2–4). Because there is no internal inertia in the model, force generated by the CE is instantaneously converted to shortening velocities at 0 s.

Influence of AFL un-latch time on power transmission

The AFL un-latch time strongly influenced the power transmitted from the MT to the load (Figs. 3 and 4). As the AFL un-latch time increased, the AFL absorbed and dissipated more and more energy. A nearly simultaneous latch (Fig. 3A) produce no negative latch power, the un-latch time produced only −22.7 mW, but reached −273 mW for the slowest AFL un-latch time (1000 ms) (Fig. 3B) and this significantly attenuated the power transferred from the MT to the load (Fig. 4A). As a consequence of the increasing latch absorption with increasing un-latch times, an AFL with a near instantaneous release (un-latch time = 10 ms; near-perfect escapement) yielded $P_{LOAD} = 839$ mW ($P_{RATIO} = 4.88$) a substantial amplification (Fig. 3A) while the slowest releasing latch (un-latch time = 1000 ms) yielded $P_{LOAD} = 86$ mW; ($P_{RATIO} = 0.43$) a substantial power attenuation (Fig. 3B).

With an AFL un-latch time of 385 ms, the trade-off between additional elastic energy stored in the SEE at the beginning of the simulation and the energy absorbed and dissipated by the AFL during release balanced out and resulted in a $P_{RATIO} = 1.0$ (Figs. 2B and 4A). For systems with an AFL, un-latch times shorter than 385 ms amplified power and un-latch times slower than 385 ms attenuated power. Thus, the threshold un-latch time for power amplification for this model was 385 ms.

Discussion

In animal movement, latches can enhance the power a MT unit transfers to its load by creating two distinct phases of energy transfer. First, in the storage phase, the latch provides a resistive force so that the CE within a MT unit can shorten slowly and store energy in series elastic tissues (SEE). Then, in the release phase, the latch acts as a switch that frees the stored elastic energy at a great rate. While we know an instantaneous latch (i.e., perfect escapement) between the storage and release phases maximizes peak power transferred to a load, we know little about how the form of the latch mediates its function. We hypothesized that, for a MT driving an inertial load an AFL with a sufficiently fast (i.e., critical) un-latching time could enhance the peak power delivered from a MT to the load beyond what is possible in the absence of a latch. We sought to characterize the critical un-latch time and evaluate whether it falls within the range of relaxation times for skeletal muscle.

In this study, we extended an already established model (Richards and Sawicki 2012) to simulate a compliant MT driving a mass across a joint with and without an AFL (Fig. 1). We used two comparisons to describe the performance of our AFLs. First, we used a base model without a latch with mass and SEE stiffness optimized to maximize peak power to the load ($P_{RATIO} = \sim 1.2$) to establish a control condition to help evaluate the performance benefits of an AFL (Fig. 2A). Then we simulated the identical

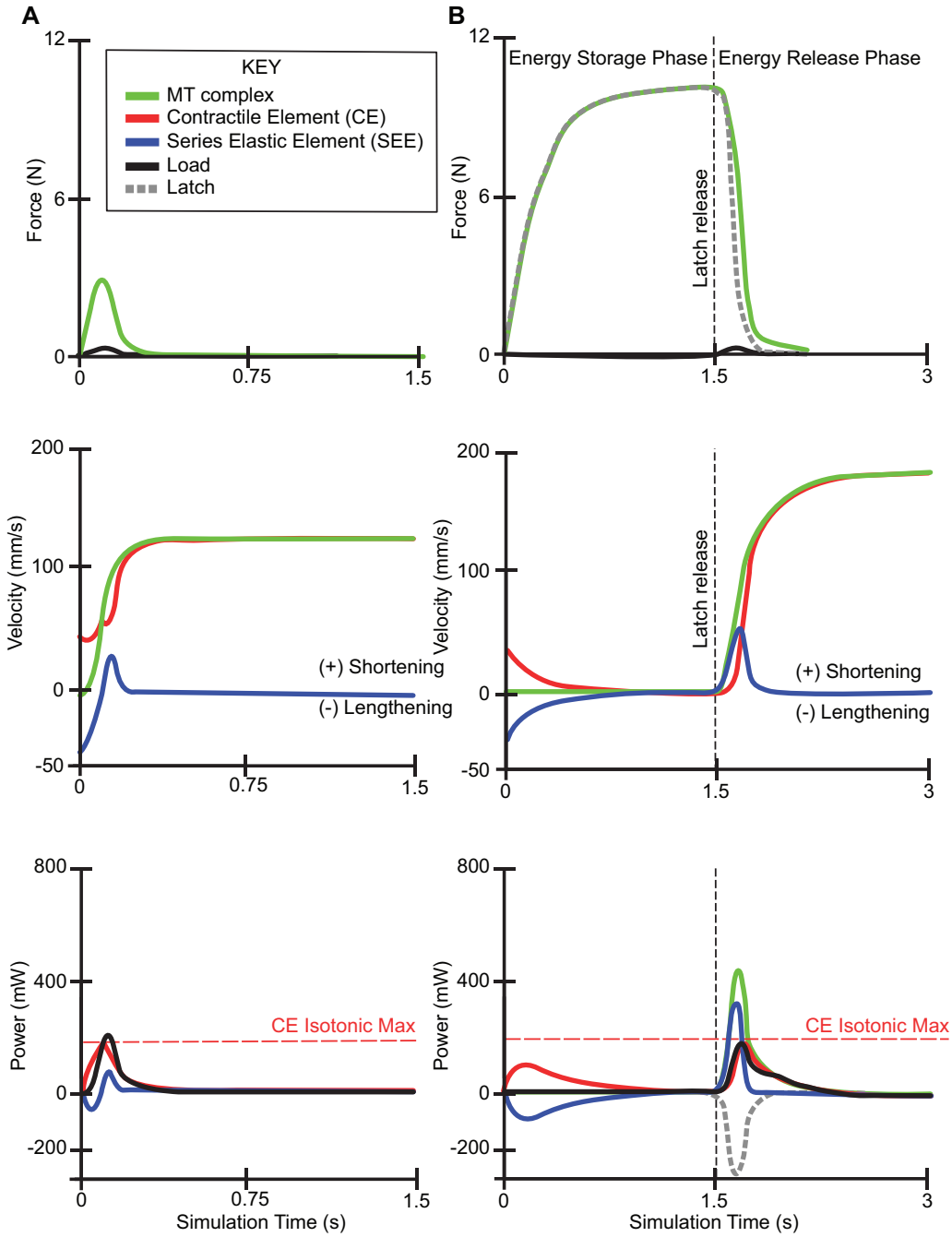

Fig. 2 Simulation output from (**A**) a system with an inertial load but no AFL and (**B**) a system with an inertial load and an AFL, distinguished by a storage phase (0–1.5 s) and release phase (1.5–3 s). Upper panels show the force on the MT unit (green), load (black), and AFL (dashed). Note that $F_{LOAD}=F_{MT}$ * EMA. Middle panels show velocity of the MT unit (green), CE (red), and SEE (blue). Upon activation at 0 s, the CE produces force and there is a non-smooth transition to instantaneous velocity because the MT has no internal inertia of its own, lower panels show mechanical power output for MT unit (green; overlapped by load in A), load (black), AFL (dashed), CE (red), and SEE (blue). The horizontal red line represents peak power for the CE *only*=172 mW. Without an AFL (A), the peak power of the load reached 203 mW, a power amplification ratio ($P_{RATIO}=P_{LOAD}/P_{CE,max}$) of ~1.2. With an AFL that un-latches in ~385 ms. (**B**) Power amplification is ~1.0, establishing the critical un-latch time for the system. With an AFL, the velocity of the CE and SEE travels in opposite directions which depicts that active CE shortening is storing energy by stretching the SEE.

system with a "perfect" latch in place using an AFL that had near-instantaneous un-latch time (10 ms) to establish the limit for peak power amplification (P_{RATIO} = ~4.88) (Fig. 3A). With these two conditions benchmarked, we explored a range of simulations with AFLs that had increasing un-latching durations up to 1000 ms (Figs. 2B, 3B, and 4). In these cases, both the MT and the AFL

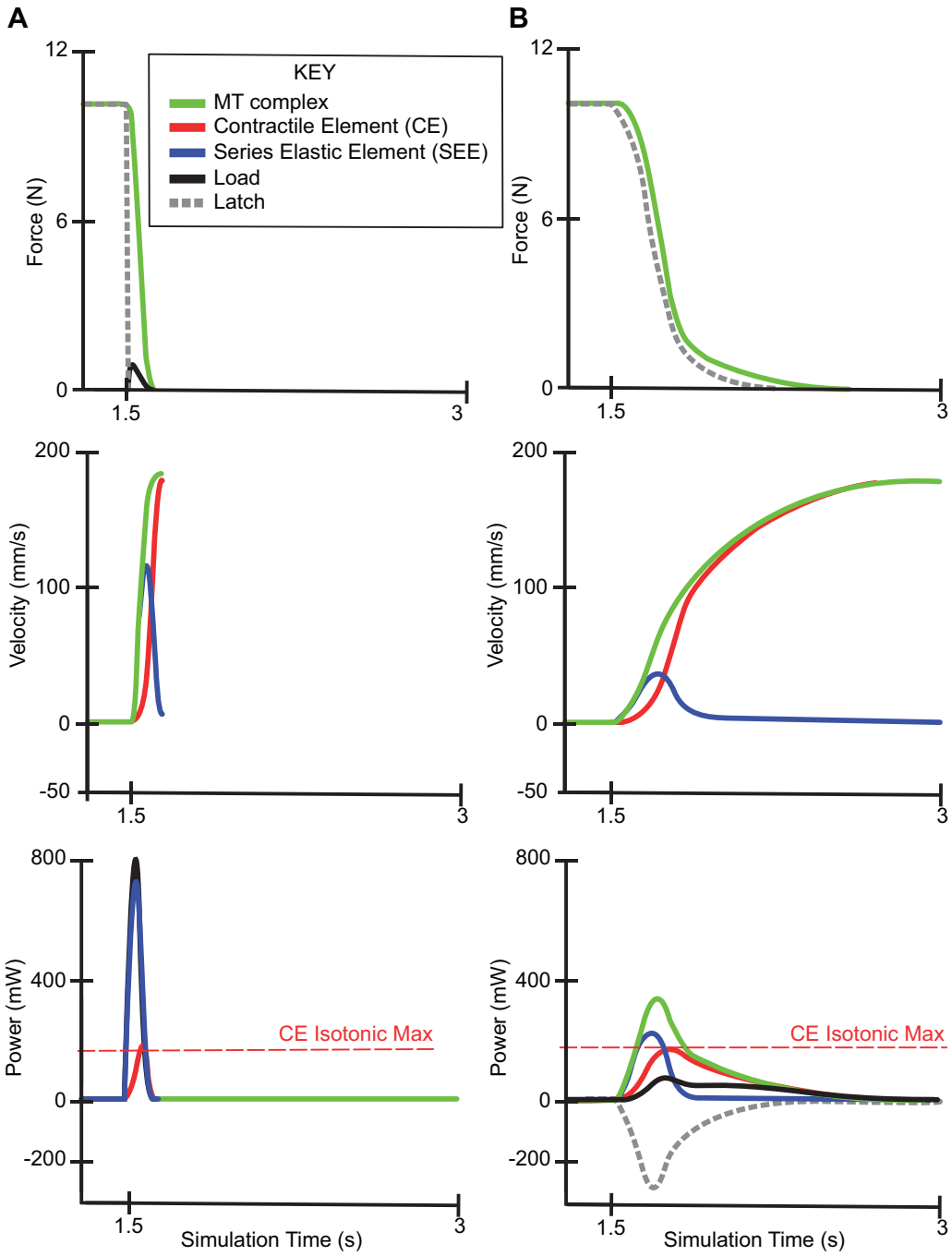

Fig. 3 Simulation output from (**A**) a system with a near-instantaneous (1 ms) AFL system and (**B**) a very slow-releasing (1000 ms) AFL. Some of the storage phase, first 1.5 s of the time series, was omitted to highlight activity in the release phase and avoid redundancy of storage dynamics. Upper panels show the force on the MT unit (green), load (black), and AFL (dashed). Note that F_{LOAD}=F_{MT} * EMA. Middle panels show velocity of the MT unit (green), CE (red), and SEE (blue). Lower panels show mechanical power output for MT unit (green; mostly overlapped by load in A), load (black), AFL (dashed), CE (red), and SEE (blue). The horizontal red line represents peak power for the CE *only*=172 mW. With a fast un-latching AFL (10 ms) (A), the peak power of the load reached 820 mW, a power amplification ratio (P_{RATIO}=P_{LOAD}/$P_{CE,max}$) of ~4.8. With a slow un-latching AFL (1000 ms) (B) peak power of the load only reached 86 mW and power is attenuated (i.e., power amplification ratio is 0.43 and <1.0).

operated across equal EMAs of 0.1. Under all circumstances, the MT was fully activated and stored the same amount of elastic energy before un-latching occurred.

As hypothesized, we found a strong relationship between AFL un-latching time and peak power transferred from the MT to the load (Fig. 4A). As un-latching time increased (i.e., slower un-latching)

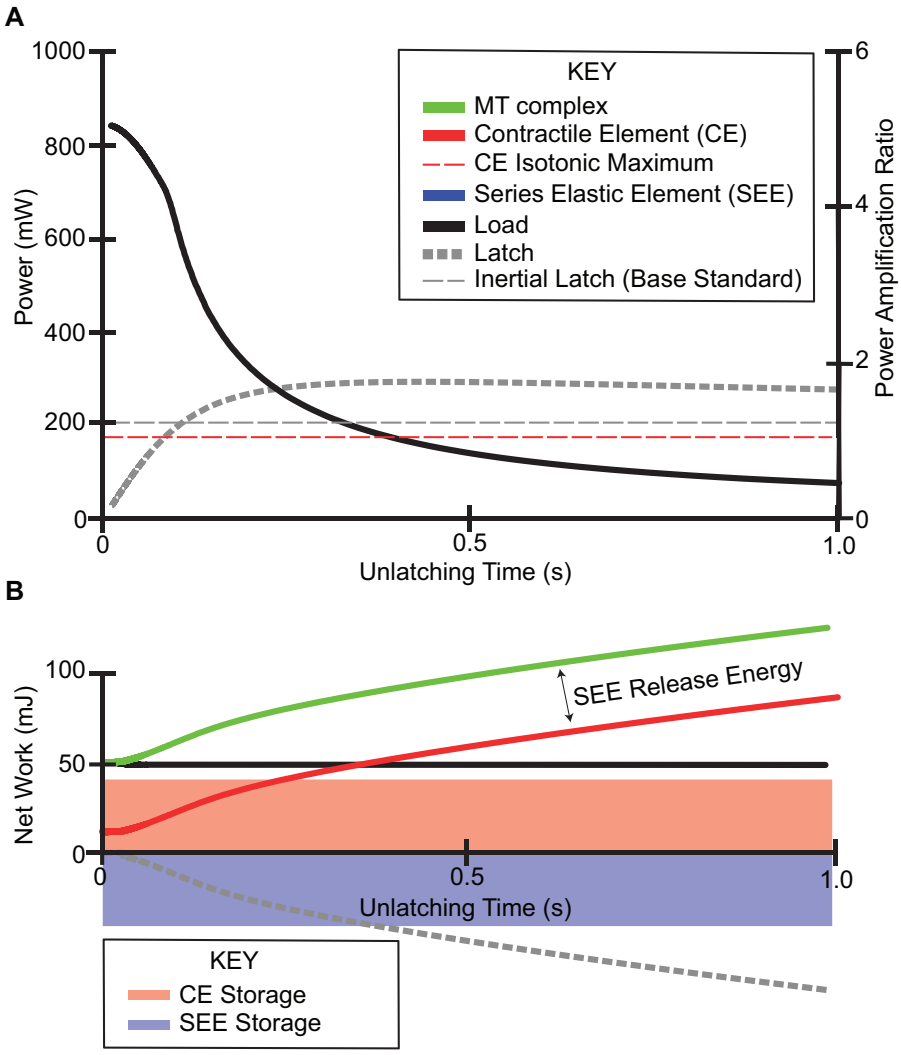

Fig. 4 **A**) Peak load power vs. AFL un-latch time. Peak power (mW) represents the rate of energy transfer to the load (black) and peak power absorbed by the latch (dashed). Horizontal lines represent maximal power produced by the CE alone ($P_{CE,max}$=172 mW; red dashed) and the inertial latch base standard (200 mW; gray dashed). As un-latch time increases peak power delivered to the load is attenuated more and more by the AFL, until the point when power amplification <1.0 at a critical un-latch time of 385 ms for this system. **B**) Net work vs. AFL un-latch time. Net work (mJ) represents the total energy generated or dissipated in the release phase as computed by integrating the power vs. time curves from the MT unit (green), CE (red), and AFL (dashed gray). The solid red area represents the amount of mechanical work transferred from the CE to the SEE during the storage phase, and this energy is released to add to the net work done by the MT on the load (SEE release energy). Note, because in this simple model, the CE does not have a defined stroke length and is not subject to force–length limitations the net work transferred to the load is constant across all simulations and dictated by the kinetic energy of the load when the CE reaches zero force at v_{max}. In this case, as AFL un-latch time increases the MT must perform more and more work to overcome AFL dissipation and produce the same net work on the load, a significant energetic penalty that negatively impacts system energy transfer efficiency.

peak power transferred from MT to load decreased. In addition, we found a critical un-latching time (385 ms for this specific system) where the AFL absorbed enough energy to cancel the amplifying effect of the pre-stored elastic energy and the system had P_{RATIO} = 1.0 (Figs. 3B and 4). Un-latching faster than the critical time amplified peak load power and un-latching slower than critical time attenuated peak load power (Fig. 4). Finally, the system with an AFL performed as well or better than the optimal system without an AFL (the base model) for un-latch time only slightly faster than critical (Figs. 2 and 4). Thus, while very simple, this model clearly highlights the importance of un-latching dynamics in shaping functional limits during high power movements. Our findings are consistent with recent studies that also found that latch release rate, prescribed by latch geometry (Ilton et al. 2018) or a critical load (Sawicki et al. 2015) is an important factor that mediates the power transferred from a

Table 1 Comparative muscle fixed-end contraction kinetics

Model (citation)	Muscle; temperature (°C)	Experience scale (F_{max})	V_{max} (muscle lengths/s)	$T_{1/2Fmax}$ (ms)	$T_{1/2\ R}$ (ms)±SE	RR
Toadfish (Rome et al. 1996)	Red trunk muscle; 16°C	Muscle bundle; F_{max} not reported	2.43±0.04	*33.46*	516±56	7.97
Toadfish (Rome et al. 1996)	White trunk muscle; 16°C	Muscle bundle; F_{max} not reported	4.12±0.29	*17.63*	*116.91*	6.63
Mouse (Askew and Marsh 1998)	Soleus; 37°C	Twitch; Tetanus; 271 kN/m^2	6.28	*4.5 ±0.2*	24.1±0.7; 37.1±1.2	5.35
Rattlesnake (Rome et al. 1996)	Shaker muscle; 16°C	Muscle bundle; F_{max} not reported	7.68±1.78	*5.91*	25.7±3.5	4.35
Rat (Close 1964)	Soleus; 35°C	*In vitro* muscle; 1.53±0.12 N	*1.52*	*18.0*	48.0±3.4	2.67
Bullfrog (Roberts and Azizi 2011)	Plantaris longus, 22°C	*In vitro* MT unit; 17.41 N	9.62±1.52 (Azizi and Roberts 2014)	*67.39*	*137.04*	2.03
Rat (Close 1964)	EDL, 35°C	*In vitro* muscle; 2.19±0.29 N	*4.27*	6.25	8.0±0.7	1.28[a]
Human (van Leemputte et al. 1999)	Elbow flexor muscles; body temperature	*In vivo* MT group; 57.0±6.9 Nm	Not reported	*111.0*	127.0	1.14[a]
Toadfish (Rome et al. 1996)	Superfast swimbladder; 16°C	Muscle bundle; F_{max} not reported	11.8±0.8	*5.76*	*5.77*	1.00[a]
Model	Critical muscle-based latch (385 ms)	≥10 N	9.0	166 (Fig. 2B)	225	1.35

[a]Muscles that may have kinetics appropriate to act as an antagonist latch according to our mathematical framework (gray).
RR, relaxation ratio is the half-relaxation time $T_{1/2R}$ divided by the time to half-peak tension $T_{1/2Fmax}$. Italicized measurements were calculated by the authors from published contraction time-series data.

MT to a load. Muscle properties that were not used in our model may affect the critical latch time. For example, muscles have internal inertia which could decrease the maximum shortening velocity and thus its power output (Günther et al. 2012; Ross and Wakeling 2016). If less power was transferred to the load in all latching simulations, it may stand to reason that a critical un-latch release rate would be <385 ms (Fig. 4).

While we did explicitly not specify the source of the AFL, we were interested in evaluating whether the un-latch times we found were within the physiological ranges of vertebrate muscle relaxation times. Muscle relaxation is the decline in force production after the neural impulse stops, or deactivates, due to calcium re-uptake into the sarcoplasmic reticulum (Periasamy and Kalyanasundaram 2007). Many factors such as fiber type, temperature, prescriptive hormones, parvalbumin, electric stimulation, and disease affect the regulation of calcium re-uptake (Salmons and Vrbová 1969; Wiles et al. 1979; Stein et al. 1982; Muntener et al. 1995; Olberding et al. 2017). Thus, there is a wide physiological range of skeletal muscle relaxation rates. Generally, physiologists use "half-relaxation time" ($T_{1/2R}$), or the time it takes force to decrease to half its value, to characterize the kinetics of muscle relaxation. Table 1 consolidates $T_{1/2R}$ for a wide range of taxa with a range of 6–516 ms. Comparably, our modeled half-unlatching times ranged from 0 to 500 ms (Fig. 4).

Absolute half-relaxation time may be significantly affected by temperature or muscle preparation size. Therefore we also compared the relative value of half-relaxation time divided by the time to half-peak tension ($T_{1/2\text{-}Fmax}$) reported as a relaxation ratio (RR; Table 1). With our model we identified that an AFL that can unload 0.4–1.2 times $T_{1/2\text{-}Fmax}$ will amplify peak power transmitted from an MT to an inertial load. Generally, vertebrate muscles relax much more slowly than they produce force (Table 1). The fastest vertebrate muscle known, toadfish superfast acoustic swimbladder, have a RR of 1.0 which is much larger than our model's instantaneous unlatch RR of 0.4. However, muscle-based latches with relaxation rates in the biological range of rat ankle extensors or human elbow flexors (e.g., 1.28 and 1.14) may still enhance power. Because our threshold value is biologically relevant both in absolute and relative terms, it may be feasible that muscles act as AFLs in nature.

The mechanism of a muscle-based latch has several benefits and trade-offs to consider. One of the

biggest benefits of a muscle-based latch would be its controllability. Latches that function with escapement (e.g., exoskeletons of arthropods) function as an all-or-none switches and can be difficult to control without a pre-planned, feedforward motor command (Kagaya and Patek 2016). Jumping insects like leafhoppers and fleas likely rely on tuned latches and springs to minimize jerk (Sutton and Burrows 2011; Bonsignori et al. 2013) and SEE stiffness appears to be evolutionarily tuned for the amount of preparatory time an animal has before take-off (Rosario et al. 2016). On the other hand, a latch that is triggered by muscle deactivation could be interrupted and or modulated on-line, within a movement by re-activating the muscle serving as the latch. One trade-off of this benefit in terms of controllability is that it would come with a metabolic penalty, because modulating activation is not free.

We note that the current study focused mostly on peak power rather than net work transferred to the load. This was in part due to the fact that net work done on the load was hard to study in this model because it remained constant, independent of unlatch time (Fig. 4B). This was due to a limitation of not constraining the CE force output by a stroke length or force–length penalties, which may be especially important in jumping systems (Roberts and Azizi 2011). Thus, it is unclear whether or not an antagonist muscle latch system would also allow controllability of net work transferred to a load (e.g., total jump distance). We acknowledge our model neglects other muscular properties in addition to the force–length relationship particularly the force–depression phenomenon in shortening muscle (Herzog et al. 2000).

We endeavored to use a generic antagonist force with logistic decay to explore hypothetical effects of latches with muscle-like relaxation dynamics. While we used biologically relevant parameters, there are several limitations to note that should be considered when interpreting or extending our results. First, we did not model our AFL as a muscle with Hill-type properties. Incorporating a Hill-type model to capture the force production dynamics of the antagonist latch may be a futile attempt. Hill-type muscle models, while common, are poor predictors of lengthening muscle force output (Harry et al. 1990). In addition, not only would a muscle-based latch be stretching, but it would also be relaxing-conditions that are rarely investigated in combination. And lastly, a Hill-type model may lessen the broad applications of this model. As is, this mathematical system could be modulated to be more specific to other power amplifying mechanisms such as ballistic feeding (Lappin et al. 2006; Deban et al. 2007) or the cam mechanisms now utilized by engineering groups building small, superfast robots (Kovač et al. 2008). In addition, the model we used for the SEE may be limited. Ilton et al. (2018) have begun focusing attention away from the CE and refocusing attention on the mechanical behavior of springs which also have force–velocity trade-offs. In fact, especially when recoiling rapidly, non-ideal springs lose energy by moving their own internal mass (inertia) and to heat loss/hysteresis. Thus, our predictions of power amplification may be an overestimate because we used an idealized Hookean spring as the SEE.

What would be the implications of an actual antagonist muscle latch? During the energy release phase, a real antagonist muscle latch would be deactivating (decrease in force production) while being stretched by the agonist. This could be broadly characterized as an eccentric contraction due to the semi-active nature of the stretch. In this dynamic state, the internal inertia, parallel elasticity, and force enhancement contributions of titin could increase the total resistive force of the antagonist muscle. Thus, this would absorb energy away from the action of the agonist. This is a rather large and complicated parametric space to test. It follows that the best method to test whether a muscle could act as an antagonist muscle latch would be with an empirical benchtop *in vitro* muscle preparation. While it seems as though realistic muscle properties may generally reduce the amount of power transmitted to the load, there are morphological variations that could mitigate these limitations. For example, fiber pennation allows fibers to rotate during stretches thus the total length of the antagonist muscle could lengthen faster than the antagonist fibers lengthen (Azizi and Roberts 2014). This means that there may be less contribution of parallel elasticity or force enhancement. Feasibility of antagonist muscle latches has also been intimated by data presented by Roach et al. (2013). Here, researchers demonstrate that human shoulders may use elastic energy storage to produce high power outputs. Specifically, the biceps muscle may act as an antagonist muscle latch while pectoralis major loads elastic energy (Roach et al. 2013).

Aside from the Hill-type parameters of the MTs themselves, there are a number of other aspects of the system that we did not study which could significantly alter the power transferred to a load. First, the load in our system comprised a mass *only*, but it is well known that load dynamics (e.g., the addition of gravity or drag) can impact MT power output

(Galantis and Woledge 2003; Richards and Sawicki 2012). Second, in our model we activated the agonist long enough to store the maximum elastic energy in the SEE before un-latching. If the AFL had un-latched prior to maximal energy storage, the system would have had less energy available to amplify the agonist MT power output (Sawicki et al. 2015; Rosario et al. 2016). Next, our model assumed an equal EMA between the agonist MT and AFL. *In vivo* systems generally have different EMAs on different sides of a joint, and these EMAs change dynamically with limb extension—a feature that could greatly impact the timing of energy transfer and therefore peak MT and load power output.

In conclusion, it is clear that latch mechanisms can increase the peak power transferred by a MT actuator to its load, but ideal escapement mechanisms with instantaneous un-latching capability lack controllability. Using a mathematical model we investigated the feasibility to use skeletal muscles as AFLs to enhance transfer of mechanical power from a MT to an inertial load. Specifically, we investigated how AFL un-latching duration enhances or attenuates the mechanical power produced by a muscle (CE) and spring (SEE) driving a mass at a fixed EMA. This foundational framework identified a critical AFL un-latch time (385 ms) at which peak load power is attenuated for slower and amplified for faster unlatching times. More interestingly however, the critical un-latch time is about ~1.35× the RR and suggests that many skeletal muscles in vertebrates including rats, frogs, cats, and humans could serve as AFLs to improve energy transfer during powerful movements. It remains unclear how other factors such as complex muscle properties, MT morphology, transmission properties (EMA), or the nature of the load (i.e., body size and environment dynamics) may affect the critical un-latch time as it relates to peak power and net work delivered from MT to load. Thus, further avenues of integration that can account for the complicated dynamics of antagonist muscles acting across the same joint (e.g., force–length, history dependence, and dynamics of lengthening de-activating MTs) will be crucial to establish the functional limits of muscle-based latches. AQ4

Acknowledgments

The authors thank Mike Rosario and Jeffrey Olberding for organizing the symposium *Playing with Power: Mechanisms of Energy Flow in Organismal Movement* at the 2019 annual meeting of the Society of Integrative and Comparative Biology in Tampa, FL, and inviting us to present this work. Sheila Patek, Christine Wall, and Laksh Kumar Punith provided many useful comments and suggestions for improving the analysis, interpretation, and presentation of the results. Finally, we thank Shelia Patek and her MURI team for organizing the workshop on small, high acceleration systems that preceded the SICB 2019 meeting as it provided useful perspectives that helped us broaden our discussion. AQ5

References

Aerts P. 1998. Vertical jumping in *Galago senegalensis*: the quest for an obligate mechanical power amplifier. Philos Trans R Soc B Biol Sci 353:1607–20.

Alexander RMN. 2002. Tendon elasticity and muscle function. Comp Biochem Physiol A Mol Integr Physiol 133:1001–11.

Askew GN, Marsh RL. 1998. Optimal shortening velocity (V/Vmax) of skeletal muscle during cyclical contractions: length–force effects and velocity-dependent activation and deactivation. J Exp Biol 201:1527–40.

Astley HC, Roberts TJ. 2012. Evidence for a vertebrate catapult: elastic energy storage in the plantaris tendon during frog jumping. Biol Lett 8:386–9.

Azizi E, Roberts TJ. 2014. Geared up to stretch: pennate muscle behavior during active lengthening. J Exp Biol 217:376–81.

Bennet-Clark HC. 1975. The energetics of the jump of the locust *Schistocerca gregaria*. J Exp Biol 63:53–83.

Bennet-Clark HC, Lucey EC. 1967. The jump of the flea: a study of the energetics and a model of the mechanism. J Exp Biol 47:59–67.

Bonsignori G, Stefanini C, Scarfogliero U, Mintchev S, Benelli G, Dario P. 2013. The green leafhopper, *Cicadella viridis* (Hemiptera, Auchenorrhyncha, Cicadellidae), jumps with near-constant acceleration. J Exp Biol 216:1270–9.

Burrows M. 2011. Jumping mechanisms and performance of snow fleas (Mecoptera, Boreidae). J Exp Biol 214:2362–74.

Burrows M, Sutton GP. 2012. Locusts use a composite of resilin and hard cuticle as an energy store for jumping and kicking. J Exp Biol 215:3501–12.

Close R. 1964. Dynamic properties of fast and slow skeletal muscles of the rat during development. J Physiol 173:74–95.

Cofer D, Cymbalyuk G, Heitler WJ, Edwards DH. 2010. Neuromechanical simulation of the locust jump. J Exp Biol 213:1060–8.

Deban SM, O'Reilly JC, Dicke U, van Leeuwen JL. 2007. Extremely high-power tongue projection in plethodontid salamanders. J Exp Biol 210:655–67.

Delp SL, Loan JP. 2000. A computational framework for simulating and analyzing human and animal movement. Comput Sci Eng 2:46–55.

Farahat WA, Herr HM. 2010. Optimal workloop energetics of muscle-actuated systems: an impedance matching view. PLoS Comput Biol 6:e1000795–11.

Galantis A, Woledge RC. 2003. The theoretical limits to the power output of a muscle–tendon complex with inertial and gravitational loads. Proc R Soc B Biol Sci 270:1493–8.

Gronenberg W. 1996. Fast actions in small animals: springs and click mechanisms. J Comp Physiol A 178:727–34.

Gronenberg W, Tautz J, Holldobler B. 1993. Fast trap jaws and giant neurons in the ant *Odontomachus*. Science 262:561–3.

Günther M, Röhrle O, Haeufle DFB, Schmitt S. 2012. Spreading out muscle mass within a Hill-type model: a computer simulation study. Comput Math Methods Med 2012:1–13.

Harry JD, Ward AW, Heglund NC, Morgan DL, McMahon TA. 1990. Cross-bridge cycling theories cannot explain high-speed lengthening behavior in frog muscle. Biophys J 57:201–8.

Heitler WJ. 1974. The locust jump: specializations of the metathoracic femoral–tibial joint. J Comp Physiol 89:93–104.

AQ6

Herzog W, Leonard TR, Wu JZ. 2000. The relationship between force depression following shortening and mechanical work in skeletal muscle. J Biomech 33:659–68.

Hogan N. 1985. The mechanics of multi-joint posture and movement control. Biol Cybern 52:315–31.

Ilton M, Bhamla MS, Ma X, Cox SM, Fitchett LL, Kim Y, Koh J, Krishnamurthy D, Kuo C, Temel FZ, et al. 2018. The principles of cascading power limits in small, fast biological and engineered systems. Science 360:eaao1082.

Kagaya K, Patek SN. 2016. Feed-forward motor control of ultrafast, ballistic movements. J Exp Biol 219:319–33.

Kovač M, Fuchs M, Guignard A, Zufferey JC, Floreano D. 2008. A miniature 7g jumping robot. Proceedings of the IEEE Internation Conference on Robotics and Automation. p. 373–8.

AQ7

Lappin AK, Monroy JA, Pilarski JQ, Zepnewski ED, Pierotti DJ, Nishikawa KC. 2006. Storage and recovery of elastic potential energy powers ballistic prey capture in toads. J Exp Biol 209:2535–53.

Lipfert S, Gunther M, Renjewski D, Seyfarth A. 2014. Impulsive ankle push-off powers leg swing in human walking. J Exp Biol 217:1831.

Marsh RL. 1994. Jumping ability of anuran amphibians. Adv Vet Sci Comp Med 38:51–111.

Muntener M, Kaser L, Weber J, Berchtold MW. 1995. Increase of skeletal muscle relaxation speed by direct injection of parvalbumin cDNA. Proc Natl Acad Sci U S A 92:6504–8.

Nishikawa KC, Monroy JA, Uyeno TE, Yeo SH, Pai DK, Lindstedt SL. 2012. Is titin a "winding filament"? A new twist on muscle contraction. Proc R Soc B Biol Sci 279:981–90.

Olberding JP, Scales JA, Deban SM. 2017. Movements of vastly different performance have similar underlying muscle physiology. J Exp Biol 220:938.

Patek SN, Baio JE, Fisher BL, Suarez AV. 2006. Multifunctionality and mechanical origins: ballistic jaw propulsion in trap-jaw ants. Proc Natl Acad Sci U S A 103:12787–92.

Patek SN, Korff WL, Caldwell RL. 2004. Biomechanics: deadly strike mechanism of a mantis shrimp. Nature 428:819–20.

Patek SN, Nowroozi BN, Baio JE, Caldwell RL, Summers AP. 2007. Linkage mechanics and power amplification of the mantis shrimp's strike. J Exp Biol 210:3677–88.

Peplowski MM, Marsh RL. 1997. Work and power output in the hindlimb muscles of Cuban tree frogs *Osteopilus septentrionalis* during jumping. J Exp Biol 200:2861–70.

Periasamy M, Kalyanasundaram A. 2007. SERCA pump isoforms: their role in calcium transport and disease. Muscle Nerve 35:430–42.

Powers K, Joumaa V, Jinha A, Moo EK, Smith IC, Nishikawa K, Herzog W. 2017. Titin force enhancement following active stretch of skinned skeletal muscle fibres. J Exp Biol 220:3110–8.

Richards CT. 2011. Building a robotic link between muscle dynamics and hydrodynamics. J Exp Biol 214:2381–9.

Richards CT, Sawicki GS. 2012. Elastic recoil can either amplify or attenuate muscle–tendon power, depending on inertial vs. fluid dynamic loading. J Theor Biol 313:68–78.

Roach NT, Venkadesan M, Rainbow MJ, Lieberman DE. 2013. Elastic energy storage in the shoulder and the evolution of high-speed throwing in *Homo*. Nature 498:483–6.

Roberts TJ. 2016. Contribution of elastic tissues to the mechanics and energetics of muscle function during movement. J Exp Biol 219:266–75.

Roberts TJ, Azizi E. 2011. Flexible mechanisms: the diverse roles of biological springs in vertebrate movement. J Exp Biol 214:353–61.

Roberts TJ, Marsh RL. 2003. Probing the limits to muscle-powered accelerations: lessons from jumping bullfrogs. J Exp Biol 206:2567–80.

Rode C, Siebert T, Blickhan R. 2009. Titin-induced force enhancement and force depression: a "sticky-spring" mechanism in muscle contractions? J Theor Biol 259:350–60.

Rome LC, Syme DA, Hollingworth S, Lindstedt SL, Baylor SM. 1996. The whistle and the rattle: the design of sound producing muscles Sonic fibers (Toadfish and Rattlesnake). Physiology 93:8095–100.

Rosario MV, Sutton GP, Patek SN, Sawicki GS. 2016. Muscle–spring dynamics in time-limited, elastic movements. Proc R Soc B Biol Sci 283:20161561.

Ross SA, Ryan DS, Dominguez S, Nigam N, Wakeling JM. 2018. Size, history-dependent, activation and three-dimensional effects on the work and power produced during cyclic muscle contractions. Integr Comp Biol 58:232–50.

Ross SA, Wakeling JM. 2016. Muscle shortening velocity depends on tissue inertia and level of activation during submaximal contractions. Biol Lett 12:10–3.

Salmons S, Vrbová G. 1969. The influence of activity on some contractile characteristics of mammalian fast and slow muscles. J Physiol 201:535–49.

Sawicki GS, Sheppard P, Roberts TJ. 2015. Power amplification in an isolated muscle–tendon unit is load dependent. J Exp Biol 218:3700–9.

Stein RB, Gordon T, Shriver J. 1982. Temperature dependence of mammalian muscle contractions and ATPase activities. Biophys J 40:97–107.

Sutton GP, Burrows M. 2011. Biomechanics of jumping in the flea. J Exp Biol 214:836–47.

Tomalka A, Rode C, Schumacher J, Siebert T. 2017. The active force–length relationship is invisible during extensive

eccentric contractions in skinned skeletal muscle fibres. Proc R Soc B Biol Sci 284:pii: 20162497.

van Leemputte M, Vandenberghe K, Hespel P. 1999. Shortening of muscle relaxation time after creatine loading. J Appl Physiol 86:840–4.

van Soest AJ, Bobbert MF. 1993. The contribution of muscle properties in the control of explosive movements. Biol Cybern 69:195–204.

Vogel S. 2005. Living in a physical world III. Getting up to speed. J Biosci 30:303–12.

Wang K, McCarter R, Wright J, Beverly J, Ramirez-Mitchell R. 1993. Viscoelasticity of the sarcomere matrix of skeletal muscles. The titin-myosin composite filament is a dual-stage molecular spring. Biophys J 64:1161–77.

Wiles CM, Young A, Jones DA, Edwards RH. 1979. Muscle relaxation rate, fibre-type composition and energy turnover in hyper- and hypo-thyroid patients. Clin Sci 57:375–84.

Wilson AM, Watson J, Lichtwark GA. 2003. A catapult action for rapid limb protraction. Nature 421:35–36.

Author Query Form

Journal: *Integrative and Comparative Biology*
Article Doi: 10.1093/icb/icz141
Article Title: Hurry Up and Get Out of the Way! Exploring the Limits of Muscle-Based Latch Systems for Power Amplification
First Author: Emily M. Abbott
Corr. Author: Gregory S. Sawicki

AUTHOR QUERIES – TO BE ANSWERED BY THE CORRESPONDING AUTHOR

The following queries have arisen during the typesetting of your manuscript. Please click on each query number and respond by indicating the change required within the text of the article. If no change is needed please add a note saying "No change."

AQ1: Please confirm whether the minor edits made in the article title is correct.

AQ2: Please check that all names have been spelled correctly and appear in the correct order. Please also check that all initials are present. Please check that the author surnames (family name) have been correctly identified by a pink background. If this is incorrect, please identify the full surname of the relevant authors. Occasionally, the distinction between surnames and forenames can be ambiguous, and this is to ensure that the authors' full surnames and forenames are tagged correctly, for accurate indexing online. Please also check all author affiliations.

AQ3: Please confirm whether the affiliations are OK as set.

AQ4: Permission to reproduce any third party material in your paper should have been obtained prior to acceptance. If your paper contains figures or text that require permission to reproduce, please confirm that you have obtained all relevant permissions and that the correct permission text has been used as required by the copyright holders. Please contact jnls.author.support@oup.com if you have any questions regarding permissions.

AQ5: Please provide a Funding statement, detailing any funding received. Remember that any funding used while completing this work should be highlighted in a separate Funding section. Please ensure that you use the full official name of the funding body, and if your paper has received funding from any institution, such as NIH, please inform us of the grant number to go into the funding section. We use the institution names to tag NIH-funded articles so they are deposited at PMC. If we already have this information, we will have tagged it and it will appear as coloured text in the funding paragraph. Please check the information is correct.

AQ6: Please confirm whether the edits made in Heitler (1974) are OK.

AQ7: Please provide the publisher and location details of Kovač et al. (2008).

AQ8: Figures have been placed as close as possible to their first citation. Please check that they have no missing sections and that the correct figure legend is present.

AQ9: These figures are currently intended to appear online in colour and black and white in print. Please reword the legend/text to avoid using reference to colour. Alternatively, please let us know if you wish to pay for print colour reproduction or to have both versions in black and white. The standard charge for colour reproduction in print is £350/e525/$600 per figure. Please check the black and white versions at the end of the paper and contact us if you have any concerns. If there are no color figures in your article, please ignore this query